IAC-14,A6,P,48x26173

DERIVING A PRIORITY LIST BASED ON THE ENVIRONMENTAL CRITICALITY

Christopher Kebschull[a], J. Radtke[a], H. Krag[b]

[a]*Institute of Aerospace Systems, Technische Universität Braunschweig, Hermann-Blenk-Str. 23, 38108 Braunschweig, Germany*
[b]*Space Debris Office, ESA/ESOC, Robert-Bosch-Str. 5, 64293 Darmstadt, Germany*

Abstract

The collision of Iridium 33 and Cosmos 2251 as well as the fragmentation of Fengyun 1C showed the consequences such events can have for the space debris environment. In order to avoid future fragmentations disused satellites and rocket bodies should be removed from orbit to reduce the buildup of new space debris, as suggested by the Space Debris Mitigation Guidelines. For objects that are posing great risk of being fragmented and thus generating new fragments, but are unable to maneuver, active debris removal missions can be considered. Such elaborate and costly missions have to be planned carefully so they unfold the required effect on the space debris environment. For the selection of target objects priority lists can be compiled, ranking the objects by urgency of removal. The ranking of the objects depends on the criteria that are chosen to be applied. For example it is common to estimate the flux an object is exposed to, or based on its mass the impact it has on the environment when fragmented, or even a combination of both. In this paper a criteria called environmental criticality (EC) is used to generate a new priority list based on the current catalogue of on orbit objects. The EC is defined as a product of the risk of fragmentation and the impact the fragmentation has on the space debris environment. Because the impact on the overall population for the given time span of 300 years is evaluated an analysis of the fragmentation in every year is necessary. This approach puts great computational constraints on the traditional Monte-Carlo based simulations of the future space debris environment. For this reason a new simulation tool based on an analytical model, which has been developed at the Institute of Aerospace Systems, is used to estimate the impact of a given fragmentation on the future space debris environment. A metric for the interpretation of the results of the criticality is proposed. The ranking objects is compared to lists, which have been derived based on different criteria.

Keywords: Priority list, Active debris removal, Space debris, Evolution, Analytical model

I INTRODUCTION

Currently many studies are focusing on how to stabilize the space debris environment in the low Earth orbit (LEO). Simulations show that objects have to be removed actively in order to reach the goal to slow down the increase or completely reverse the generation of new fragments. Numbers ranging from 5 to 10 debris objects per year have to be removed from their respective orbits using Active Debris Removal (ADR) missions [1]. These kind of missions are costly and thus have to be planned carefully [2] [3]. Their success and efficiency in reaching the stated goal is paramount. It will affect how the LEO can be used by future generations. Before setting out to start such a mission one first step is to determine which objects to remove. Different criteria can be used to derive such a priority list. A simple approach is to determine the collision flux on the target objects and derive their collision risk in order to reach the conclusion how likely it is for the objects to be fragmented. This can be further modified to incorporate the object's mass to get an idea on how the consequences of a fragmentation on the space debris environment would be. A similar relation has been used in [4] to retrieve the given priority list. While this gives a good idea on which objects may be the main drivers for the fragment generation it does not take into account that the target objects

Email address: c.kebschull@tu-braunschweig.de (Christopher Kebschull)

are moving through a dynamically changing debris environment or may have a different impact on the environment when fragmenting in different altitudes. This and the remaining orbital lifetime (ROL) of the object can alter the list significantly, as will be shown in this paper. Sec. II will cover the definition of the new criteria for deriving a new priority list, which will be discussed in Sec. IV. To overcome the computational demands the criteria puts on current space debris evolution models like LUCA (**L**ong-term **U**tility for **C**ollision **A**nalysis) an analytical model has been derived and implemented. This will be introduced briefly in Sec. III.

II ENVIRONMENTAL CRITICALITY

In order to overcome the shortcoming of the simple approach stated above a new criteria has been defined. It is called the environmental criticality (EC). It is able to give a combined statement about the risk an object on orbit is subjected to and the impact its fragmentation would have on the environment. The criticality is an indicator that describes how harmful an object may be to its environment. The definition of the criticality is separated in two parts, a risk and an impact component:

$$C_{crit} = c_{risk} \cdot c_{impact}. \tag{1}$$

In detail this forms the following cumulative relation for a simulation over a given timeframe:

$$C_{crit} = \sum_{t=t_{start}}^{t_{end}} \left[c_{risk,t} \cdot \sum_{\tau=t_{frag}}^{t_{end}} (\Delta p \cdot \Delta\tau) \right], \tag{2}$$

where the formulation of the criticality demands the evaluation of the change in the collision flux in all orbital regions after a fragmentation has occurred:

$$c_{risk,t} = \Phi \cdot A \cdot t. \tag{3}$$

Φ is the collision flux, A as the cross sectional area of the target object and t the elapsed time of the simulation. As part of the c_{impact} component of the Eq. 2 again with Φ as the collision flux for the basic scenario in which no fragmentation has occurred and the current scenario, where the target object as been fragmented and its fragments have spread, Δp is defined as:

$$\Delta p = p_{frag} - p_{no\ frag} = \left(\Phi_{frag} - \Phi_{no\ frag}\right) \cdot A \cdot t. \tag{4}$$

Additionally the $\Delta\tau$ term factors in the time that has passed since the fragmentation occurred. The risk portion of the equation ($c_{risk,t}$) considers the collision rate of the target object for each step of the simulation time. The impact, expressed as an integral, over the timeframe from the beginning of the fragmentation to the end of the simulation, determines the change in the overall collision rate. The overall collision rate is the collision rate in each cell of the environment.

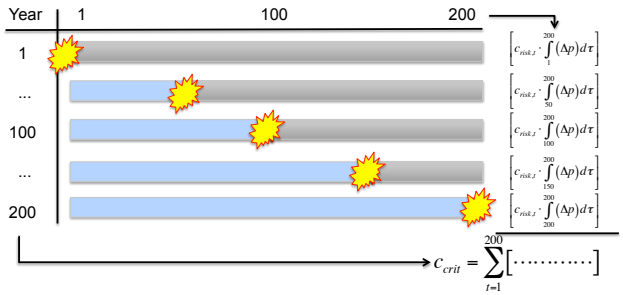

Fig. I: The EC respects the influence a fragmentation has on every region in LEO. A target object is fragmented in every possible epoch and its influence is analyzed by comparing the collision rate before and after the collision in every succeeding year (Δp). The risk of fragmentation is also part of the equation, determining the probability of the fragmentation just before it is triggered.

Fig. I shows an example computation of the EC of an arbitrary target object. The simulation evaluates the influence of the object over a time span of 200 years. In the first year the risk for the object ($c_{risk,t}$) is evaluated through the collision rate using the background scenario that has been prepared initially. Following is a triggered fragmentation. An entire population is generated for the next 200 years (gray bar). In every year the difference in the collision rate Δp is determined through a comparison of the fragmentation scenario and the background scenario. In the following year this process is repeated. The background population, which is stored as snapshots per epoch, is loaded, the collision rate of the target object is determined, the object is fragmented and the 199 years until the end of the simulation timeframes are generated through the Population Generator. Each of these 199 epochs is analyzed. This process is repeated for each year in the desired 200 year simulation time span. In the last simulation year the fragmentation is triggered, and only that year is used for an analysis of the criticality. The cumulated criticality (also environmental criticality) value is derived as a sum over all criticality values of the 200 year simulation time span. This process is computationally very expensive due to the fact that the Population Generator has to create 199 scenarios of the future space debris environment following the fragmentation of the target object at each epoch on its decaying orbit. The simulation is cut short only when the target object enters the atmosphere. The last value of the EC is then valid for the given simulation time span.

For this special case a longer simulation time span would not change the EC. Generally however a variation of the simulation time span alters the outcome of the EC values. Thus the EC is only comparable when it is derived with the same simulation settings.

III ANALYTICAL APPROACH

Using the usual numerical approach requires so much computational power that a single evaluation of the EC over a 200 year time frame takes months. For this reason an analytical model has been derived and implemented. The low Earth orbit is partitioned into 34 altitude shells and 67 eccentricity shells. Objects from 10 cm to 100 m sizes are considered. To further simplify the model only two object categories are regarded: intact bodies like satellites and rocket bodies and fragments originating from explosion and collision events. Both categories are distinguished by their assumed area-to-mass ratio. The individuality of the objects is lost in the process of moving them into altitude shells, eccentricity and diameter bins. No further information about the object but what category it originates from is kept. The model regards known effects that cause the dynamic behavior of the space debris environment based on source and sink mechanisms. Launches and fragmentations are considered as sources. The natural decay, PMD as well as ADR measures are regarded as sinks. For the generation of fragments due to explosions and collisions a modified implementation of the NASA Breakup Model [5] is used. In order to be able to influence the model behavior fitting parameters have been designed into the equations. For example the drag coefficient c_D for the intact bodies and fragment objects can be defined by the user. Similar models have been derived before [6] [7]. In [8] the model is described in more detail.

III.1. Implementation

The prototype implementation of the defined model is named SANE, which stands for **S**imple **An**alytical **E**volution. While the simulation of the future space debris environment is the central part of the implementation it is merely the means to accomplish a greater goal, which is to retrieve information on the influence a fragmentation of a given target object has on the evolution of the environment. There are two available modes that can be used when running SANE. The first mode is the Population Generator. It forecasts the space debris environment over the timeframe. It uses a simple explicit Euler integrator to produce the snapshots for each year of the simulation. In this mode the number of outputs are generated that show the distribution of the intact bodies and fragments over the cells of the LEO. This can be up to 27 336 cells (default settings with a combination of 34 altitude shells, 12 diameter bins, 67 eccentricity classes), depending on the configuration of the simulation. In the current state the natural decay sink mechanism is managed through the residence time of the two kinds of objects (intact bodies and fragments) in a given altitude shell and eccentricity bin. The residence times are available as lookup tables and can easily be exchanged against different ones in the data folder of the simulation. Parameters for the different source and sink mechanisms like the collision and explosion scaling factors can be set in the configuration files. In the Population Generator mode SANE can be fitted against the more complex numerical models by comparing the produced results and altering the parameters in the configuration files. In the current state the lookup tables and fitting parameters have been set that SANE is able to reproduce space debris forecasts and collision flux values based on results produced by LUCA, a tool developed at the Institute of Aerospace Systems.

The second mode available is the Criticality Computation that relies on the first mode. It generates the different space debris environment scenarios based on the time of the target object fragmentation, as described in Sec. II. In this mode the impact of each of the fragmentation scenarios is analyzed by determining the change in the collision rate in each of the 27 336 cells by comparing it to the no-fragmentation scenario. Based on the number of objects in an altitude shell, SANE can derive the collision flux. A linear relation between the number of objects in a given altitude and the flux has been derived using MASTER-2009. The flux then can be used to derive the EC for a given target object in accordance with eq. 2. SANE is able to forecast the space debris environment for 200 years in about 120 seconds, which results in a duration of about 2 hours of the EC computation for one target object. A more detailed look into the implementation of SANE is given in [9] and [10].

III.2. Debris Environment

In the Population Generator mode SANE is able to forecast the space debris environment and deliver the appropriate output so that its performance can be analyzed. Based on the settings derived after fitting SANE against LUCA Fig. II shows a forecast of the intact bodies environment for the year 2200. It is visible that SANE can follow the overall trend. The characteristic objects numbers with peaks at around 775 km, 975 km and 1450 km altitude are visible. The growth over the simulation time in these areas is comparable. However SANE shows a constant overestimation of the 775 km altitude shell while the shells below are underestimated. This might be the case due to the binning effects so that the intact bodies are not moving ”smooth” enough through the al-

titude shells. The decay in the areas below 775 km seems to be too high or the decay in the 775 km altitude shell is not high enough. The region around 975 km altitude is underestimated for the same reason; due to the dynamic environment the objects are moving too fast into lower altitude shells or are not moving fast enough into this altitude shell from the one above. The highest difference in object numbers at the end of the simulation can be found in the 1325 km altitude shell with an object discrepancy of 252 objects. The standard deviation over the altitude shells is at 85.45, while the overall relative discrepancy is at 73 %. The highest relative discrepancy can be found in the 1275 km altitude shell with a 812 % difference in the number of intact bodies. While LUCA predicts 22 objects, SANE estimates 197. When looking at the evolution of the intact bodies in higher altitude shells it is apparent that there is room for optimizing the decay data set. The decay is too high for the 1425 km and 1475 km altitude shells, which results in an increase of objects in the adjacent altitude shells. Adapting the passage times in the provided files of SANE could have the desired effect. Alternatively the decay correction coefficient c_D for intact bodies can be altered. In Fig. III the

Fig. II: Evolution of the intact bodies over time when considering launches and natural decay only in comparison to results from LUCA for the year 2200.

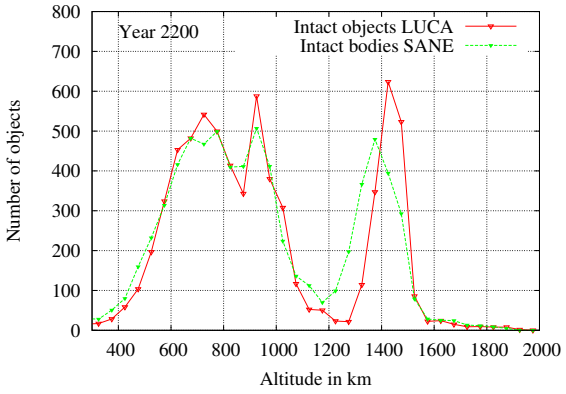

collision module has been enabled. This time however the fragments of the future population are compared. As with the intact bodies SANE can follow the overall trend that LUCA derives in a complex numerical computation. Two peaks at 750 to 800 km altitude and around 1400 km altitude are visible. The discrepancy over all altitude shells is at 39 %, the standard deviation is at 73.82 fragments. The highest absolut discrepancy at the end of the simulation can be found in the 675 km altitude shell. The biggest relative discrepancies can be found toward the lower boundaries of the model, in the 300 km and 350 km altitude shell with a relative error of 254 % and 212 % deviation. While SANE predicts 16 and 27 fragments in those altitudes LUCA determines that 4 and 9 fragments respectively should be there. Due to the small number of objects the high relative error is enabled.

Fig. III: Evolution of the fragments over time when considering launches and natural decay as well as collisions in comparison to results from LUCA for the year 2200.

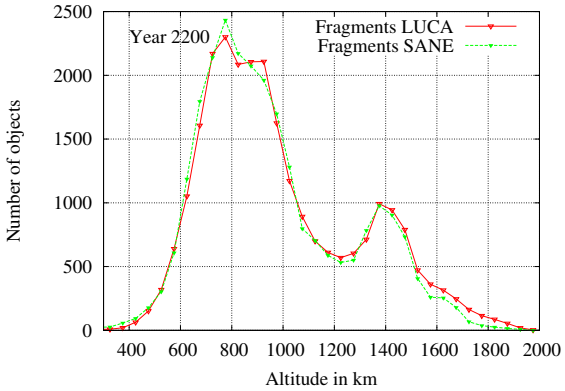

III.3. Collision Flux

From the total number of objects in a given cell SANE is able to determine the collision flux based on a linear relation that has been derived by looking at the development of the space debris environment in each altitude shell retrieved from MASTER-2009. The reference epochs 1990, 1996, 2001, 2005 and 2009 have been taken into account for this analysis. Fig. IV shows the results that are achieved with this approach. The collision flux on two reference objects is shown over a 200 year simulation time in comparison with LUCA results. It is visible that the collision flux derived by SANE can follow the trend over time, even though that over- and underestimations due to simplifications in the model occur. A short analysis in [9] shows that discrepancies up to 28 % can be observed, averaged over the simulation time. The resulting error is influenced by the fact that the flux relation stated above currently considers only one inclination bin. SANE has been optimized for 80° to 100° inclinations. When using this relation on lower inclinations an overprediction can be observed.

III.4. Environmental Criticality

The process of determining the EC leads from the number of objects determined by the Population Generator mode over the derived linear relation of the collision flux to the EC definition that demands the calculation of two different scenarios (fragmentation and

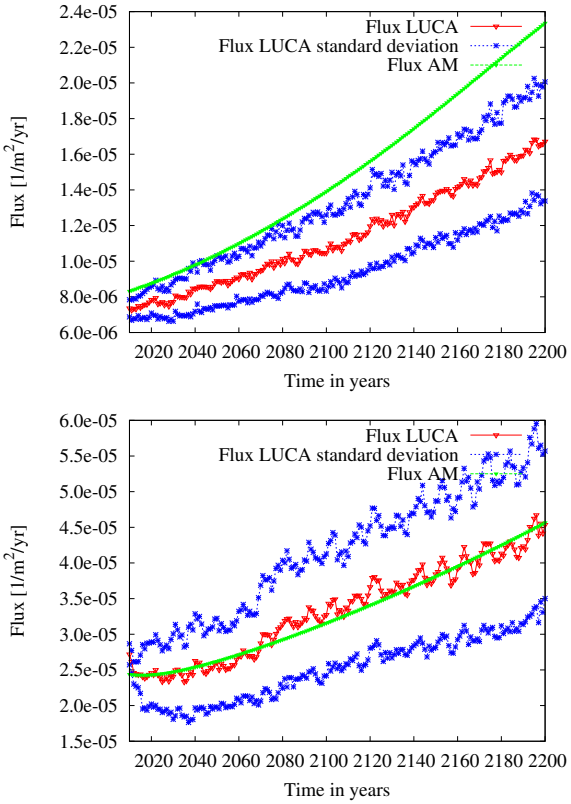

Fig. IV: Collision flux of reference objects in 63° to 65° (1) and 82° to 86° (2) inclination bins compared between LUCA and SANE.

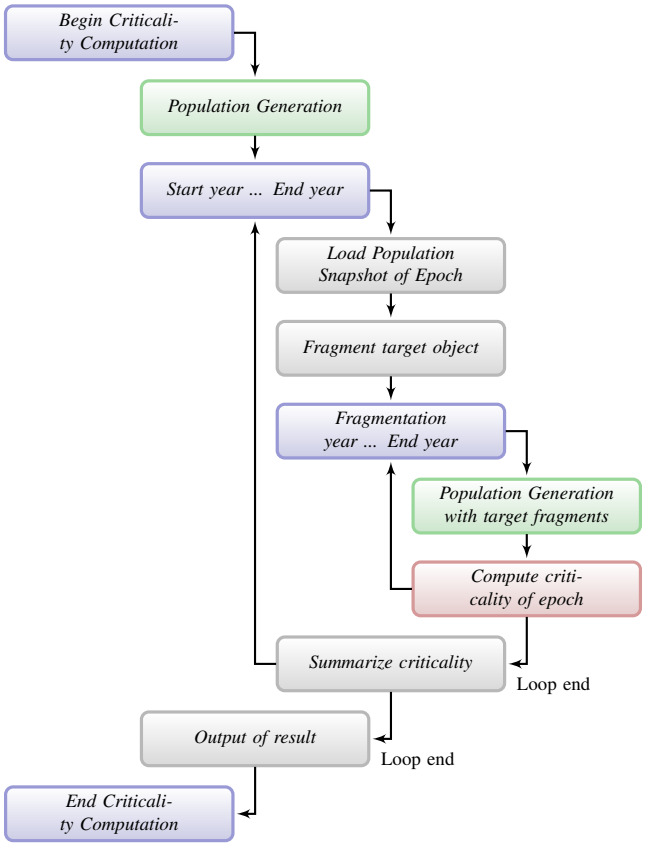

Fig. V: Details of the process for computing the environmental criticality as needed for the entire simulation span.

non-fragmentation) of the future space debris environment. Before the EC for an object is calculated a snapshot of the future space debris population is calculated and stored in memory. This image is later used to quickly load a state for a given year. This process is accomplished by the Population Generator incorporating all source and sink mechanism. After finishing the calculation for a simulation year the snapshot is stored in memory and the next year is processed based on the current one. After the last year has been processed the available data is merged and prepared for further analysis by the Criticality Computation mode.

The described process of deriving the future population is an integral part of the criticality computation. As shown in Fig. V the Population Generator (green) is used once initially to create the non-fragmentation population for the simulation time span. Once it has been generated the simulation starts and loads the first snapshot for the epoch. Within this epoch the target object is fragmented and its fragments are distributed among the LEO cells (gray). The second layer loop computes the impact the fragmentation has (expressed through the criticality) from the time of the fragmentation to the end of the simulation time span. Within this loop the Population Generator is used again to forecast the environment with the new fragments that have been added. The criticality that is derived for the given epoch (red) is based on the collision rate difference in every cell of the environment (altitude, diameter, eccentricity) between the just created environment with fragments and the initially computed non-fragmentation environment. The overall criticality (environmental criticality) is computed as a sum of all criticality results from every epoch, as shown in Eq. 2.

IV PRIORITY TARGETS

Based on the process shown in Sec. III.4 a new priority list using the EC as the criterion has been derived. The baseline of objects to be analyzed is a pre-filtered list, which has been used in the *Fragmentation Consequence Analysis Study*. The top 85 objects on the list have been processed by SANE using a 300 year simulation time span starting in 2009. Tab. I shows the ranking of the top 50 objects. The environmental criticality ranges from a value of 1.20E-02 on the low end

to 2.64E+00 on the high end. Many objects of the same mass and orbits have been determined to have the same EC. This can be observed for the Iridium objects as well as Ariane and Zenit-2 second stage rocket bodies. The reason for these groups of objects on the list are primarily the mass and orbital elements that for many of these objects are assumed to be similar. Especially from the point of view of the model, which partitions the altitude, eccentricity and diameter, the objects are in the same category and thus move through the same cells and receive the same amount of flux as well as they have the same impact on the environment. In future versions of the implementation this might change due to a more precise propagation of the object and an interpolation between the cells the objects move through. However in between these blocks of similar objects some individuals can be made out, like the satellites Envisat, METOP-A and -B, COBE, ARGOS, SPOT 3, COSMOS 2486 and NOAA 17.

Fig. VI shows the evolution of the EC value of selected objects over the simulation time. It becomes obvious that the four Zenit-2 second stage rocket bodies (red solid line) on top of the list, which have the identical criticality values due to identical masses and orbital elements that correspond to the same semi-major axis and eccentricity bins, are three times "more critical" than Envisat, which is ranked at position 5. In turn METOP-A and METOP-B, which are at position 6 and 7, only have a slightly lower criticality than Envisat. The next big offset in the list occurs at rank 14 which is COSMOS 2486 (39177). The values for this and the following 7 objects are about three times lower than SPOT-3 (22823) after a 300 year simulation time. The increase of the criticality stops once an object has entered the atmosphere. Due to the cumulative definition of the criticality it will not drop to zero but keep its last value (maximum) until the simulation ends. The figure also shows the trend that shortly

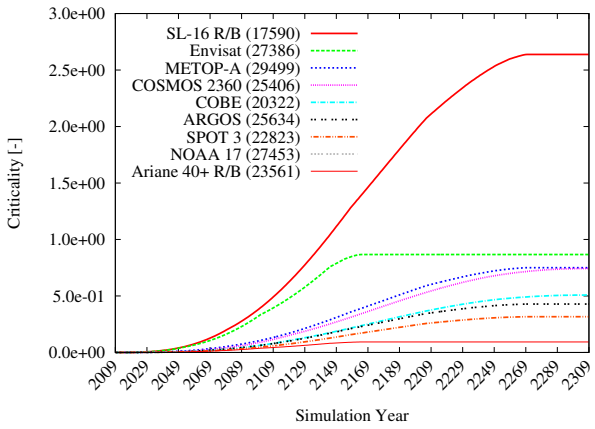

Fig. VI: Evolution of the EC of some of the top ranking objects.

Rank	Catalog#	Designation	Source	EC [-]
1	17590	Zenit-2 sec. stage	CIS	2.64E+00
2	19120	Zenit-2 sec. stage	CIS	2.64E+00
3	25400	Zenit-2 sec. stage	CIS	2.64E+00
4	25407	Zenit-2 sec. stage	CIS	2.64E+00
5	27386	Envisat	ESA	8.67E-01
6	29499	METOP-A	EUME	7.50E-01
7	38771	METOP-B	EUME	7.50E-01
8	25406	Cosmos 2360	CIS	7.43E-01
9	27421	SPOT 5	FR	5.28E-01
10	20322	COBE	US	5.08E-01
11	25394	Resurs-O2 1	CIS	4.83E-01
12	25634	ARGOS	US	4.28E-01
13	22823	SPOT 3	FR	3.16E-01
14	39177	COSMOS 2486	CIS	1.13E-01
15	27453	NOAA 17	US	9.78E-02
16	20443	Ariane 40 st. 3	FR	9.29E-02
17	21610	Ariane 40 st. 3	FR	9.29E-02
18	22830	Ariane 40 st. 3	FR	9.29E-02
19	23561	Ariane 40 st. 3	FR	9.29E-02
20	25261	Ariane 40 st. 3	FR	9.29E-02
21	26070	Zenit-2 sec. stage	CIS	4.63E-02
22	28353	Zenit-2 sec. stage	CIS	4.63E-02
23	16182	Zenit-2 sec. stage	CIS	4.17E-02
24	17974	Zenit-2 sec. stage	CIS	4.17E-02
25	19650	Zenit-2 sec. stage	CIS	4.17E-02
26	20625	Zenit-2 sec. stage	CIS	4.17E-02
27	22220	Zenit-2 sec. stage	CIS	4.17E-02
28	22285	Zenit-2 sec. stage	CIS	4.17E-02
29	22566	Zenit-2 sec. stage	CIS	4.17E-02
30	22803	Zenit-2 sec. stage	CIS	4.17E-02
31	23088	Zenit-2 sec. stage	CIS	4.17E-02
32	23405	Zenit-2 sec. stage	CIS	4.17E-02
33	23705	Zenit-2 sec. stage	CIS	4.17E-02
34	24298	Zenit-2 sec. stage	CIS	4.17E-02
35	11511	Cosmos-3M stage 2	CIS	2.85E-02
36	12443	Cosmos-3M stage 2	CIS	2.85E-02
37	16682	Cosmos-3M stage 2	CIS	2.85E-02
38	23432	Cosmos-3M stage 2	CIS	2.85E-02
39	27387	Ariane 5 sec. stage	FR	2.32E-02
40	25260	SPOT 4	FR	2.20E-02
41	24796	Iridium 4	US	1.20E-02
42	24836	Iridium 14	US	1.20E-02
43	24841	Iridium 16	US	1.20E-02
43	24870	Iridium 17	US	1.20E-02
45	24903	Iridium 26	US	1.20E-02
46	24905	Iridium 24	US	1.20E-02
47	24946	Iridium 33	US	1.20E-02
48	24948	Iridium 28	US	1.20E-02
49	24967	Iridium 36	US	1.20E-02
50	25043	Iridium 38	US	1.20E-02

Tab. I: List of objects ranked with the EC as the criteria.

after the 300 year mark COSMOS 2360 (violet dotted line) might surpass METOP-A/-B(blue dotted line), thus being "more critical" in the considered simulation timeframe. This change in the position on the priority list has occurred for COBE (cyan dash/dotted line) and ARGOS (black double dotted line) around the year 2100. Also NOAA 17 (thin gray dashed line) surpasses the Ariane 40+ rocket body (thin red solid line) just before the year 2250. For better visibility of these movements the evolution of the criticality is shown on a logarithmic scale

in Fig. VII.

Fig. VIII and IX show the cumulated criticality per

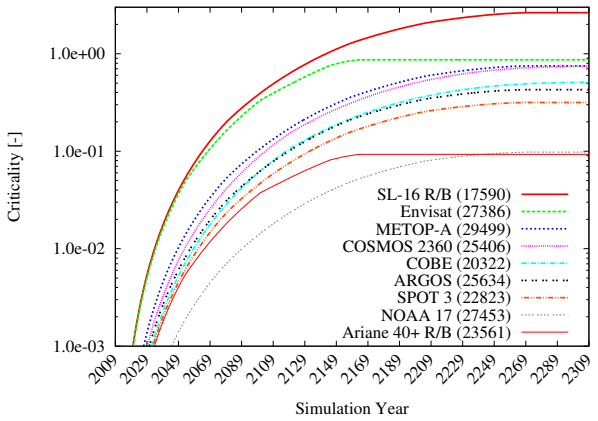

Fig. VII: Evolution of the EC of some of the top ranking objects (logarithmic scale).

year for four objects on the priority list split into its components c_{risk} and c_{impact}, as defined in Eq. 1 and the non-cumulated criticality value (which is the product of c_{risk} and c_{impact}). Generally it can be observed that the c_{risk} value is steadily increasing over the lifetime of the object, which makes sense when considering that the longer an object is subject to a harmful environment with a given possibility of collisions, the higher its risk (probability) of fragmentation. For the c_{impact} part a different behavior is observable. With the decay of the object the impact on the environment can change drastically. The lower on orbit a fragmentation occurs the lower its impact is on the environment. This is due to fragments decaying immediately when closer to the Earth's surface. Also due to the sum in Eq. 2 the time factors in from the time of fragmentation to the end of the simulation. This is an inverse behavior to the risk component which increases over time. The considered timeframe for the impact is reduced over the simulation time because the target fragmentation occurs later and later with the progression of the simulation and computation of the criticality (revisit Fig. I).

An analysis of the individual cases in Fig. VIII shows that the impact of the two Zenit-2 second stage rocket bodies (blue dotted line) is of the same magnitude. However their risk components are two orders of a magnitude apart, even though SANE predicts the same orbital lifetime. The reason for this difference is the slightly different orbit of both objects. The combination of the semi-major axis and the eccentricity brings the top 4 Zenit-2 second stage rocket bodies into shells/bins that have a higher flux than for the rest of the rocket bodies. Because SANE does not have any interpolation between cells implemented yet the movement of an object between cells

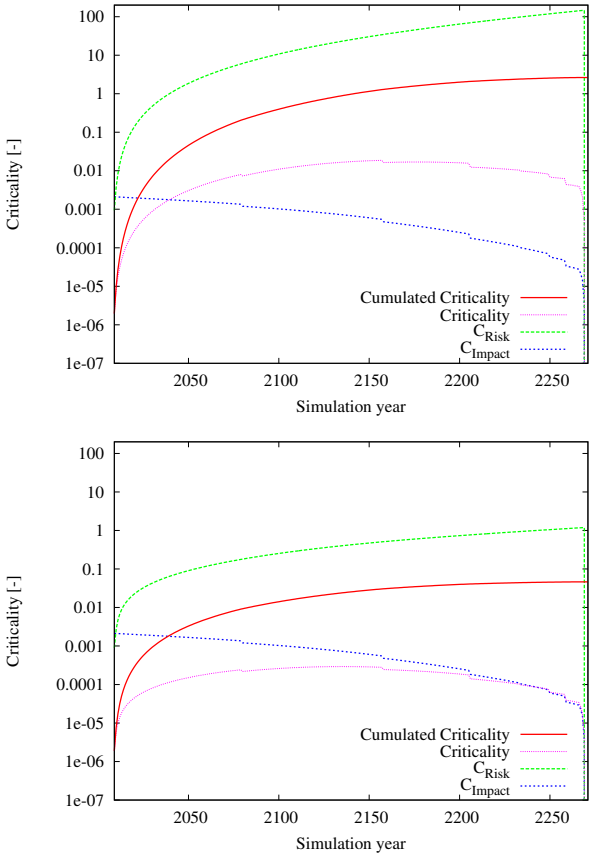

Fig. VIII: Evolution of the EC (cumulative), criticality (non-cumulative) and its two components c_{risk} and c_{impact} of the Zenit-2 second stage R/B (25700) on top and Zenit-2 second stage R/B (28353) below.

can have a big effect, which leads to an observable offset in the results, especially in the case of the impact when (due to decay) the object moves into the next lower altitude shell.

Looking at Envisat (Fig. IX) it can be observed that during its orbital lifetime it has a similar development of the criticality components than the top most Zenit-2 second stage rocket bodies. However it decays about 100 years earlier, which lets the criticality drop to zero over the rest of the simulation lifetime (The cumulative criticality, as shown in the figures below, stagnates). The Ariane 40 rocket body has the same orbital lifetime as Envisat. But due the difference in their masses the impact the rocket body has on the environment is lower. Slight differences in their orbital elements also cause the rocket body to have a lower risk. Both objects enter the Earth's atmosphere around the year 2160 and thus do not have any further impact on the LEO environment. From that point in time on the EC stagnates.

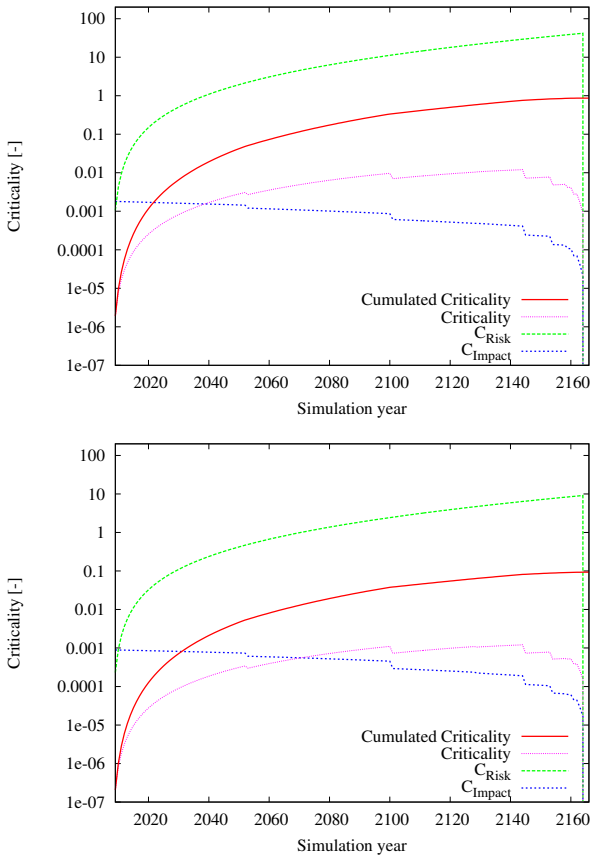

Fig. IX: Evolution of the EC (cumulative), criticality (non-cumulative) and its two components c_{risk} and c_{impact} of Envisat (27386) above and ARIANE 40 R/B (20443) below.

IV.1. Comparison

In the mentioned paper [4] and reiterated in Tab. II a list of 24 priority targets is shown, which has been compiled at the Institue of Aerospace Systems in 2012. While both approaches see various Zenit-2 rocket bodies on top of the list they disagree on the top rank of the European satellite Envisat. SANE puts it on position 5 as opposed to position 1. It can be observed that heavy objects make up the top 5 objects on both lists. However SANE moves lighter objects up while others are moved further down on the list, like the Daichi second stage (28931). This underlines that not only the mass of a target object is important but also which orbital region it moves through in the considered timeframe. SANE moves the object down to rank 77 from 22. The same can be said for the H-2A Stage 2 (27601) which is moved to rank 69 from 23. The less heavy Zenit-2 stages, with a mass of 8.2 *t*, which occupy ranks 6 to 21 on the list in [4] are moved to rank 20 and below when processed with the Criticality Computation in SANE. In between the ranks 5 and 20 satellites like METOP-A and -B as well as Cosmos 2360, SPOT 3 and 5, COBE, Resurs-O2 1, ARGOS, COSMOS 2486, NOAA 17 and various Ariane 40 stages are ranked, which are not showing up in the other list.

Rank	Catalog#	Designation	Source
1	27386	Envisat	ESA
2	28353	Zenit-2 stage 2	CIS
3	31793	Zenit-2 stage 2	CIS
4	27006	Zenit-2 stage 2	CIS
5	26070	Zenit-2 stage 2	CIS
6	25400	Zenit-2 stage 2	CIS
7	22285	Zenit-2 stage 2	CIS
8	23088	Zenit-2 stage 2	CIS
9	20625	Zenit-2 stage 2	CIS
10	22566	Zenit-2 stage 2	CIS
11	23405	Zenit-2 stage 2	CIS
12	24298	Zenit-2 stage 2	CIS
13	23705	Zenit-2 stage 2	CIS
14	16182	Zenit-2 stage 2	CIS
15	17974	Zenit-2 stage 2	CIS
16	19650	Zenit-2 stage 2	CIS
17	17590	Zenit-2 stage 2	CIS
18	25407	Zenit-2 stage 2	CIS
19	22220	Zenit-2 stage 2	CIS
20	22803	Zenit-2 stage 2	CIS
21	19120	Zenit-2 stage 2	CIS
22	28931	Daichi	JPN
23	27601	H-2A stage 2	JPN
24	19461	Titan IIG st. 2	US

Tab. II: List of objects as provided by the ILR in 2012 [4] showing the top 24 priority objects.

SANE considers the evolution of space debris environment (and thus the flux) when evaluating the possibility of fragmentation and also factors in the impact the fragmentation has on the entire environment. Also the decay of the target objects through the dynamically changing space debris environment is regarded. However especially these values are rough estimations. In SANE, just as the population itself, the target object is handed through the altitude and eccentricity shells until it enters the atmosphere. PMD measures are not considered in either approach. Also for active satellites no station keeping is regarded.

V CONCLUSION

In this paper the process chain of deriving a new list of priority targets has been shown, which is based on the environmental criticality (EC). The EC definition has

been given. Because of the formulation of the EC high computational effort is needed to retrieve a value. A computation with current numerical approaches would take months for a single object. Therefore an analytical model called SANE (**S**imple **AN**alytial **E**volution) has been developed, that is able to forecast the space debris environment in a fraction of the time numerical approaches like LUCA need, while still remaining in accordance with its numerical pendant. SANE uses source and sink mechanisms to model the space debris environment. Based on the number of objects SANE is able to estimate the collision flux, which in turn is used to compute the EC of a target object. A pre-filtered list of target objects has been processed with SANE. Using the EC as a criterion a priority list has been compiled showing the four heavy Zenit-2 stages on the ranks 1 to 4 while Envisat is on rank 5, followed by METOP-A and -B and various satellites through rank 15. Ariane 40 stages occupy ranks 16 to 20. The lighter Zenit-2 stages can then be found on the ranks 21 to 34. Also in these simulations the evolution of the criticality could be shown. Depending on the simulation time the overall EC value of an object will change, which might change its position in the priority list over time. In the executed 300 year simulations the top most Zenit-2 stages are more than three times more "critical" than the objects on the following ranks. While this elaborate approach takes a lot of computational effort simpler approaches that consider the flux and the mass of the target object only also show similar objects on the top most ranks. However these approaches usually do not take into account the decay of the target object through the dynamically changing space debris environment, which SANE is designed to do. Thus it cannot only be used to derive the EC but it can also be applied for the rapid generation of the future space debris environment. This is useful e.g. when applying parameter variations for ADR or PMD measures. This can lead to evaluations to estimate the efficiency of these measures. Another application for SANE in conjunction with a cost model plugin is the estimation of cost efficiency of ADR missions. The question of how much a reduction of a certain amount of future collision risk would cost can be answered, based on single and multiple target missions proposed in [3].

VI ACKNOWLEDGMENTS

The development of the described analytical model is a part of the project *Fragmentation Consequence Analysis for LEO and GEO Orbits* supported by ESA's General Studies Programme (contract 4000106517/12/F/MOS).

VII REFERENCES

[1] J.-C. Liou, "An active debris removal parametric study for leo environment remediation.," *Advances in Space Research*, vol. 47, pp. 1865–1876, 2011.

[2] C. Wiedemann, S. Flegel, M. Möckel, J. Gelhaus, V. Braun, C. Kebschull, M. Metz, and P. Vörsmann, "Active debris removal," No. DLRK 2012-281452, Deutscher Luft- und Raumfahrtkongress, September 2012.

[3] V. Braun, E. Schulz, and C. Wiedemann, "Cost estimation for the active debris removal of multiple priority targets," No. PEDAS.1-31-14, COSPAR, August 2014.

[4] C. Wiedemann, S. Flegel, M. Möckel, J. Gelhaus, V. Braun, C. Kebschull, J. Kreisel, M. Metz, and P. Vörsmann, "Cost estimation of active debris removal," No. IAC-12.A6.5.3., International Astronautical Congress, 2012.

[5] N. L. Johnson, P. H. Krisko, J.-C. Liou, and P. D. Am-Meador, "Nasa's new breakup model of evolve 4.0," *Advances in Space Research*, vol. 28, no. 9, pp. 1377–1384, 2001.

[6] A. Rossi, A. Cordelli, P. Farinella, and L. Anselmo, "Collisional evolution of the earth's orbital debris cloud," *Journal of Geophysical Research*, vol. 99, pp. 23,195–23,210, November 1994.

[7] H. G. Lewis, G. G. Swinerd, R. J. Newland, and A. Saunders, "The fast debris evolution model," *Advances in Space Research*, vol. 44, pp. 568–578, 2009.

[8] C. Kebschull, V. Braun, S. Flegel, B. Reihs, S. Hesselbach, J. Gelhaus, M. Möckel, J. Radtke, C. Wiedemann, H. Krag, and P. Vörsmann, "A simplified approach to analyze the space debris evolution in the low earth orbit," No. IAC-13,A6,2,3x19121, 64th International Astronautical Congress, September 2013.

[9] C. Kebschull, P. Scheidemann, S. Hesselbach, J. Radtke, V. Braun, and H. Krag, "Simulation of the space debris environment in leo using an analytical approach," No. PEDAS.1-0011-14, COSPAR, August 2014.

[10] S. Hesselbach, C. Kebschull, J. Radtke, V. Braun, P. Scheidemann, and H. Krag, "An analytical approach to describe the effects of collisions and explosions in the low earth orbit," No. PEDAS.1-0011-14, COSPAR, August 2014.